photochem

MDPI

Article

E–Z Photoisomerization in Proton-Modulated Photoswitchable Merocyanine Based on Benzothiazolium and o-Hydroxynaphthalene Platform

Aleksey A. Vasilev [1,2,*], Stanislav Baluschev [3,4], Sonia Ilieva [1] and Diana Cheshmedzhieva [1,*]

[1] Faculty of Chemistry and Pharmacy, Sofia University "Saint Kliment Ohridski", 1 James Bourchier Blvd., 1164 Sofia, Bulgaria; silieva@chem.uni-sofia.bg
[2] Institute of Polymers, Bulgarian Academy of Sciences, Akad. G. Bonchev St., bl 103A, 1113 Sofia, Bulgaria
[3] Faculty of Physics, Sofia University "Saint Kliment Ohridski", 5 James Bourchier Blvd., 1164 Sofia, Bulgaria; balouche@mpip-mainz.mpg.de
[4] Max Planck Institute for Polymer Research, Ackermannweg 10, 55128 Mainz, Germany
* Correspondence: ohtavv@chem.uni-sofia.bg (A.A.V.); dvalentinova@chem.uni-sofia.bg (D.C.); Tel.: +35-92-8161-354 (D.C.)

Abstract: The potential of *E–Z* photoisomerization in molecular organic light-to-thermal conversion and storage in an *E*–styryl merocyanine system was studied in a polar acidic medium. A photoswitchable styryl merocyanine dye (*E*)-2-(2-(2-hydroxynaphthalen-1-yl)vinyl)-3,5-dimethylbenzo[*d*]thiazol-3-ium iodide was synthesized for the first time. The reversible *E–Z* photoisomerisation of the dye was investigated using UV-Vis spectroscopy and DFT calculations. *E–Z* isomerization was induced through the use of visible light irradiation (λ = 450 nm). The obtained experimental and theoretical results confirm the applicability of the *Z* and *E* isomers for proton-triggered light harvesting.

Keywords: *E–Z* photoisomerization; spiropyran; organic light-to-thermal systems; merocyanine dyes; DFT

Citation: Vasilev, A.A.; Baluschev, S.; Ilieva, S.; Cheshmedzhieva, D. *E–Z* Photoisomerization in Proton-Modulated Photoswitchable Merocyanine Based on Benzothiazolium and o-Hydroxynaphthalene Platform. *Photochem* **2023**, *3*, 301–312. https://doi.org/10.3390/photochem3020018

Academic Editors: Marcelo Guzman, Vincenzo Vaiano and Rui Fausto

Received: 2 May 2023
Revised: 28 May 2023
Accepted: 9 June 2023
Published: 19 June 2023

1. Introduction

Photoswitchable molecules have been widely investigated due to their potential applications as light-responsive materials. Several classes of organic compounds that can undergo reversible photoisomerization around double bonds (C=C, C=N, N=N) are reported in the literature. The common denominator in these systems is that one of the conformers is thermodynamically stable, and the other is metastable and is formed after irradiation with UV or visible light [1,2]. Examples of photoswitchable molecules include dihydroazulene/vinylheptafulvene (DHA/VHF) [3,4], fulvalene dimetal complexes [5], norbornadiene/quadricyclane (NBD/QC) [6], and azobenzene systems [1,2,7–11]. Qiu et al., provide an overview of recent developments and applications of various types of synthetic photoswitches as molecular solar thermal (MOST) energy storage materials [11]. The application of azobenzenes performing *E–Z* photoisomerization upon irradiation is driven by their possible inclusion as light-triggered switches in polymers, surface-modified materials, proteins, and a variety of "molecular machines" [7,12]. Azobenzenes are highly valued photoswitches with applications in biological systems due to the fact that the photoisomerisation process is fast and they have a high photoisomerization quantum yield [2]. Diarylethene molecules, for example, can be converted from a conjugated to a cross-conjugated state upon illumination in the visible region, and this reversible isomerization is the basis of room-temperature conduction switching [13,14]. The class of spiropyrans is among the most important photochromes, with broad applications as smart materials in energy, data storage and photopharmacology [15–18].

The photochromism of spiropyrans is due to the interconversion between the ring-closed spiropyran (SP) structure and ring-open merocyanine (MC) form, in which the

C−O bond is split [17]. The photochemical properties of the two isomers are quite different, making spiropyrans unique as a class of photoswitches. Their applicability to new spiropyran-based dynamic materials is determined by the fact that the molecules undergo a reversible and continuous interconversion in response to variety of stimuli. Spiropyran functionalized materials have been developed due to their potential applications [18]. The fluorescent properties of spiropyran-bound polymers have been studied extensively due to their potential applications in detection and imaging. PULSAR microscopy has been developed with a special application for imaging biological systems and overcoming the significant problem of false positive signals due to cell autofluorescence [19,20]. The functionalization of biomolecules with spiropyran molecular photoswitches contributes to solving various scientific challenges, such as the light-assisted control of natural biological properties [21,22], the photoregulation of enzyme activity [23], and others.

The protonation of the o-hydroxyl group in merocyanines built by 3,3′-dimethylindolenine and phenol end groups has been broadly investigated [24–29]. Acidochromism has been reported to modify the thermally induced conversion to the protonated merocyanine form (MCH+) [24–29]. However, the mechanism and nature of the intermediates formed throughout these reports are not consistent. Fissi et al. [24] and Wojtyk et al. [25], for example, observed that an equilibrium between the non-protonated and the protonated spiropyran is established in the presence of trifluoroacetic acid, lying in favor of the protonated E-merocyanine form. In another report, Rémon et al. [26] proposed that, in an aqueous medium, the protonation only occurs at a pH below 0.5 and that the only protonated species present is the open-ring merocyanine form, which is in thermal equilibrium with the non-protonated closed form. Additionally, Schmidt et al. [27] also noted the formation of the protonated E-merocyanine in ethanol upon the addition of trifluoroacetic acid. Overall, these reports denote that ring opening to the stable protonated E-merocyanine occurs in a strongly acidic environment. In other words, it was postulated that a rapid equilibrium is established between species of the transient spiropyran forms that have a broken Cspiro-O bond and a geometry intermediate to the perpendicular spiro and the planar merocyanine form under sufficiently acidic conditions [24–27]. In the same period, Roxburgh et al., reported the trifluoroacetic acid induced the thermal ring-opening of spiropyrans to their protonated E isomer that was proposed to be via either the unprotonated or protonated Z form [28]. The proposed intermediacy of the protonated Z form was subsequently supported by Shiozaki, who proposed that the protonation of spiropyran in ethanol with sulfuric acid, a stronger acid than trifluoroacetic acid, generated the Z-merocyanine form, which could not only undergo subsequent thermal but also photochemical Z/E isomerization [29]. Shiozaki's interpretation of the changes observed by UV-vis absorption spectroscopy, analogous to the acid-induced ring opening (C-O bond cleavage) observed for the related photochromic spirooxazines [29], which was supported by theoretical results. Kortekaas et al. [30] demonstrated that the extent of acid-induced ring opening is controlled by matching both the concentration and strength of the acid used. The authors show that with strong acids, full ring opening to the Z-merocyanine isomer occurs spontaneously, allowing its characterization via 1H NMR spectroscopy as well as UV/vis spectroscopy. The reversible switching between Z-E isomerization through irradiation with UV and visible light is considered. Under sufficiently acidic conditions, both E- and Z-isomers are thermally stable. The judicious choice of the acid so that its pKa lies between that of the E- and Z-merocyanine forms enables thermally stable switching between spiropyran and E-merocyanine forms, and hence pH-gating between thermally irreversible and reversible photochromic switching. Our group recently demonstrated [31] for the first time the *E*–*Z* photoisomerization observed directly by excitation with light, substantially red-shifted compared to the absorption spectrum of the *E*–*Z* active moieties via the process of triplet–triplet annihilation upconversion. As photoactive molecular systems, we used a series of rare-earth-free stabilized styryl dye-Ba^{2+} complexes prepared via an improved, easy, reliable two-step synthetic procedure. The goal is to find molecular systems that do not contain metals and are environmentally friendly. Therefore, our

efforts have been focused on finding metal-free photoswitchable molecules operating in the visible region (450–600 nm) and testing their ability in terms of proton-triggered *E*–*Z* photoisomerization. We are looking for a metastable structure that is the Z-form, which should thermally relax to the E-isomer. Usually, the Z-form is higher in energy and more unstable. The transition from Z- to E-form is expected to result in energy gain.

The aim of the present study is to investigate the *E*–*Z* photoisomerization of merocyanine (*E*)-2-(2-(2-hydroxynaphthalen-1-yl)vinyl)-3,5-dimethylbenzo[d]thiazol-3-ium platform as a molecular organic light-to-thermal conversion system in acidic conditions. We synthesized and investigated the photophysical properties of a promising candidate, which is easy to obtain and that can be subsequently modified via structural changes.

2. Results and Discussion

2.1. Synthesis

The Knövenagel type condensation of the CH-acid 2,3,5-trymethyl-benzothiazolium iodide (***1***) and a slight molar excess of 2-hydroxy-1-napthaldehyde (**2**) in the presence of catalytic amounts of N,N′-diisopropyl-ethylamine (DIPEA) afforded the reaction product ***3*** in very good yield (71%), Scheme 1. The reaction conditions were modified, thus leading to the complete conversion of reactant ***1*** and the easy purification of the target product ***3***. Only one spot on the TLC was observed after the separation of the reaction product from the ethanol/ethyl acetate solution. Single recrystallization from ethanol/ethyl acetate afforded the target dye ***3*** in analytical purity.

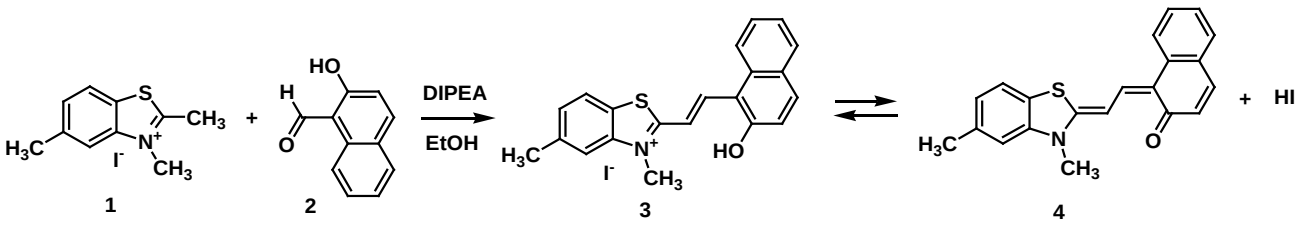

Scheme 1. Synthesis of the photochromic dye ***3*** and its merocyanine tautomer ***4***.

The chemical structure of dye ***3*** was proved via NMR spectroscopy, ESI-MS spectrometry, melting point and UV-VIS spectroscopy. In the proton NMR spectrum of protonated merocyanine **3** in DMSO-d_6 (Figures S1–S3), all of the characteristic signals of the proposed chemical structure are observed. At 2.52 ppm, a singlet with integral intensity corresponding to three protons is denoted. In our opinion, it corresponds to the methyl group attached to the aromatic core of the benzothiazolium fragment. In a weaker field at 4.06 ppm, a singlet with integral intensity for three protons appears, which corresponds to the methyl protons of the group directly bonded to the quaternary nitrogen atom of the methyl-benzothiazolium fragment. The doublet at 7.01 ppm with a J-constant of 9.2 Hz is characteristic of the methine proton of the styryl group connecting the two aromatic moieties of the conjugated system of the dye. The other similar methine proton signal appears at 7.84 ppm with the same J-constant as the previous one. In the aromatic part of the proton signals, the most characteristic is the singlet appearing at 7.89 ppm, describing the proton between the methyl group of the benzothiazlium fragment and the quaternary nitrogen atom. The number and integral intensity of the remaining signals corresponds to the protons in the aromatic part of dye structure **3**. The presence of only positive signals in the carbon DEPT spectrum of dye **3** (Figure S4) certifies the absence of methylene protons in the structure and confirms the presence of methyl and methine protons, corresponding to the proposed chemical structure. The signals at 21.65 ppm and 56.50 ppm can be assigned to the carbon atoms from the methyl groups.

To the best of our knowledge, dye **3** has not been described in the literature.

2.2. Photophysical Properties of Dye 3

Absorption Spectra

The electronic absorption spectra of dye ***3*** in solvents with different polarities are demonstrated in Figure 1 and Table 1. The dye displays several different bands between 300 and 600 nm. As expected [18,28], two forms of the dye are present in the solution (Figure 1). The longest wavelength absorption corresponds to the merocyanine form (***MC***) (Scheme 2). The extensive conjugation in the structure of the merocyanine dye leads to strong absorption in the visible region (574–590 nm in the studied solvents). The *trans*-styryl (***TS***) hemicyanine form (Scheme 2) is characterized by absorption maxima from 451 nm to 481 nm, depending on the solvent polarity. It can be concluded from Figure 1 that dye ***3*** exhibits horizontal and vertical sovatochromism typical for merocyanine and styryl dyes. It is well known that merocyanine dyes are characterized by positive solvatochromism, while styryl hemicyanine dyes are characterized by negative ones.

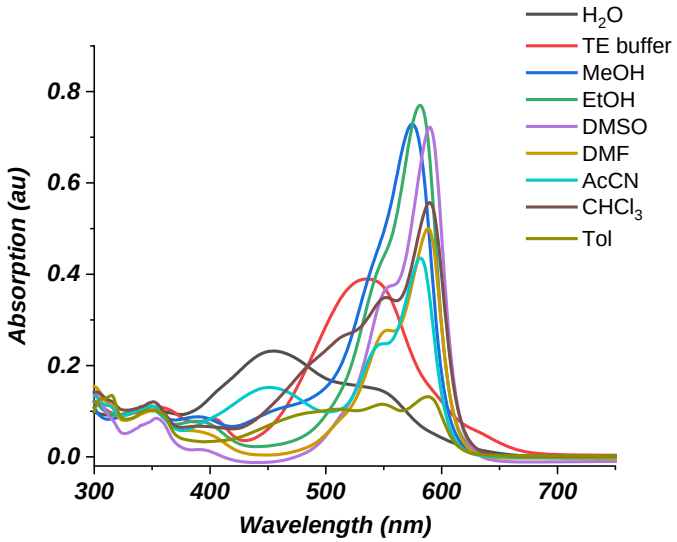

Figure 1. UV-VIS absorption spectra of merocyanine dye ***3*** in solvents with different polarity.

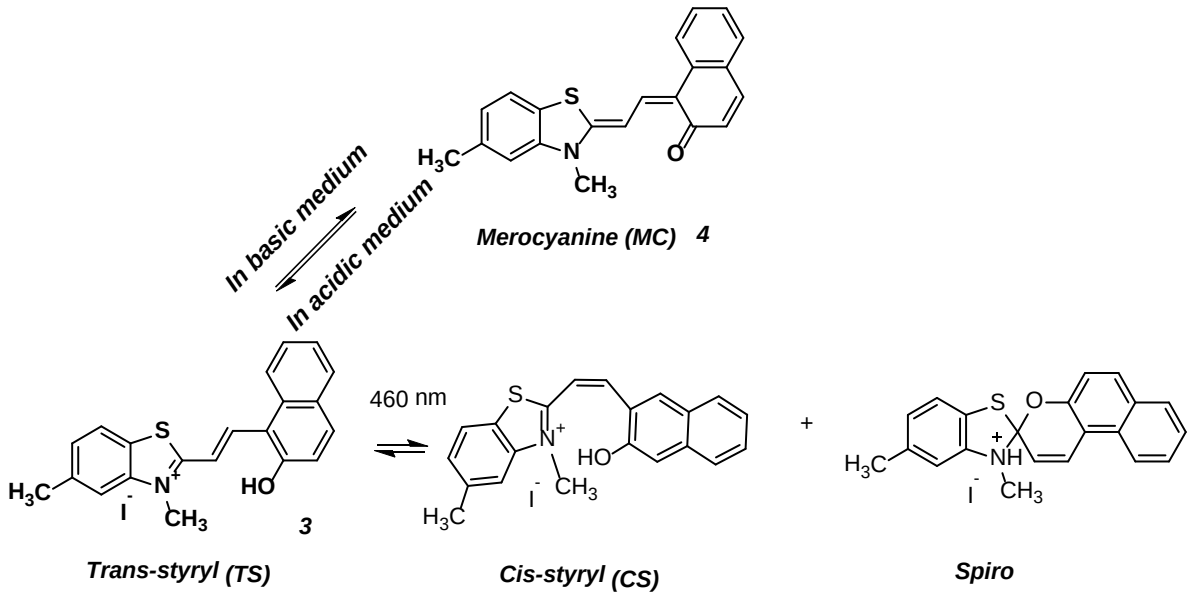

Scheme 2. Isomers of dye *3* in acidic medium.

Table 1. Dependency of the visible absorption of dye ***3*** from the solvent polarity.

Solvent	Polarity Index	Dielectric Permittivity ε	λ_{max1} (nm) Styryl	ε_1 (L × mol^{-1} × cm^{-1})	λ_{max2} (nm) MC	ε_2 (L × mol^{-1} × cm^{-1})
Toluene	2.4	2.3741	481	9 490	589	13,160
$CHCl_3$	4.1	4.71	-----	-----	590	55,700
MeOH	5.1	32.613	459	10 510	574	72,860
EtOH	5.2	24.85	-----	-----	581	76,980
Acetonitrile (AcCN)	5.8	35.688	451	15 220	582	43,540
DMF	6.4	37.219	-----	-----	588	50,050
DMSO	7.2	46.826	-----	-----	590	72,190
H_2O	10.2	78.355	454	23 180	543	14,930
TE buffer pH = 7	-----		407	6 460	535	38,960

As can be seen from Figure 1, the solvatochromism of the merocyanine form is mainly vertical (molar absorptivity from 13,160 L × mol^{-1} × cm^{-1} in toluene till 76,980 L × mol^{-1} × cm^{-1} in ethanol) with a weak red/bathochromic shift of the longest wavelength maximum going from less polar to more polar solvents. This positive solvatochromism is an indication of an increased dipole moment of the excited state relative to the ground state. Meanwhile, for the trans-styryl form, we observed a negative solvatochromism typical for dyes of the styryl cyanine type [22]. The merocyanine form predominates in some solvents (Table 1), while both forms of the dye exist simultaneously in other solvents.

Solvents, such as DMF, DMSO, ethanol, and methanol, stabilizing the merocyanine form, are more suitable for investigating the *E*-*Z* photoisomerization of dye ***3***. The acidochromic properties of dye ***3*** in DMF were investigated. DMF–an aprotic, basic, polar solvent, can coordinate acidic protons with its lone pair. Dye ***3*** was titrated with glacial acetic acid in DMF. Figure 2 shows the change in the absorption of dye ***3*** as a function of the amount of glacial acetic acid added to a solution of the dye in DMF. As the amount of added acid increases, the intensity of the absorption band at 581 nm corresponding to the merocyanine form ***4*** (***MC*** Scheme 2, Figure 2) decreases, while at the same time the intensity of the absorption band at 451 nm that corresponds to the *trans*-styryl (or so-called "protonated merocyanine") form ***3*** (***TS*** Scheme 2, Figure 2) increases. The merocyanine form converts into the protonated species, absorbing at λ_{max} 480 nm upon the addition of acid to the solution. The presence of a distinct isosbestic point is unequivocal proof of the existence of the two discussed tautomeric forms (***MC*** and ***TS***) in DMF–acetic acid solution. The merocyanine form of dye ***3*** is stable in basic medium. The addition of glacial acetic acid (AcOH) leads to the formation of *trans*-styryl ***3***.

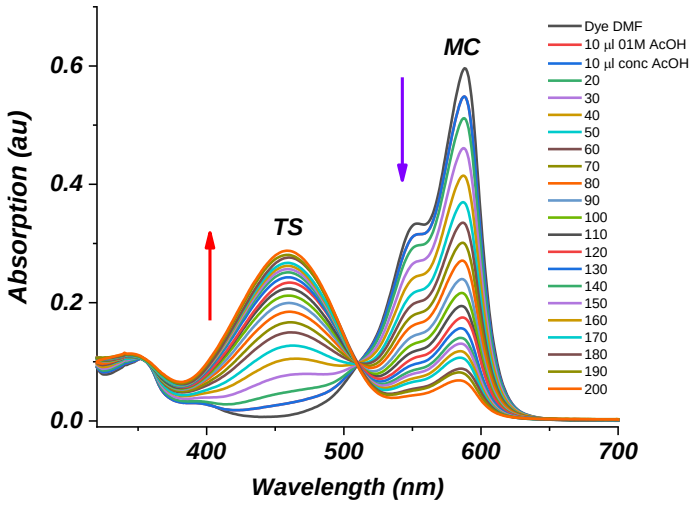

Figure 2. Acetic acid triggered merocyanine to styryl form (***3*** to ***4***) isomerization in DMF as a solvent.

The solution was irradiated with a 450 nm laser for different periods of time to induce *cis*-trans isomerization. The irradiation of the solution (dye ***3*** in DMF and acetic acid) resulted in a substantial decrease in the intensity of the band responsible for the *trans*-styryl form of the dye (Figure 3). As can be seen from Figure 3, the irradiation after the fortieth minute leads to a complete disappearance of the signals for forms ***3*** and ***4***, which is visually registered as a complete discoloration of the solution. This phenomenon is accompanied by an increase in the absorption intensity at 363 nm, which can be associated with the formation of the *cis*-styryl isomer and its eventual incorporation into a spiropyran cycle. The formation of a second isosbestic point at 390 nm (Figure 3) confirms this hypothesis. The color of the solution did not recover, and the system did not return to the original absorbance values at 450 nm, even after six months of relaxation in the dark at room temperature and/or upon heating to 50 °C. The irreversibility of the *E*–*Z* isomerization process in DMF–acetic acid makes these conditions unsuitable for the intended application.

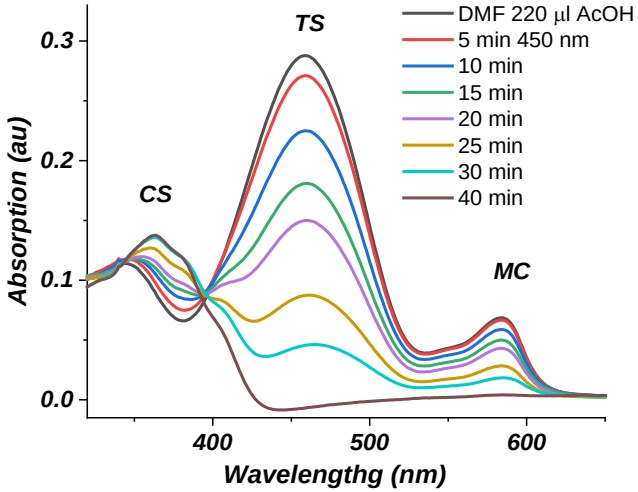

Figure 3. *E*-*Z* photoisomerization of dye ***3*** in the presence of acetic acid upon 450 nm laser irradiation.

Our goal was to achieve the transformation of the metastable *cis* form to the most stable *trans*-form upon relaxation of the system. The observations described above forced us to repeat the experiment in a different solvent and with a different acid. Since we are interested in *E*–*Z* photoisomerization of merocyanine dye ***3***, the process was studied in ethanol as a medium, and the titration was performed with concentrated hydrochloric acid.

In ethanol, the merocyanine form ***4*** is stable, as can be seen from Figure 4 (black line). Then, 1 M aqueous hydrochloric acid was added to the solution, resulting in the formation of *trans*-styryl form ***3*** (463 nm, the blue and red lines in Figure 4). In contrast to the experiment in DMF, in ethanol, even small amounts of 1 M aq. HCl acid resulted in a complete conversion of form ***4*** (***MC***) to form ***3*** (***TS***). In ethanol–water, the ***TS*** form of the dye remains stable for at least 24 h, which is a prerequisite for performing the above experiment in the given new medium (ethanol/water). In an acidic environment, the merocyanine form is eliminated and is no longer the most stable form. Even if the spiro form is formed, under these conditions, it will quickly open to the *cis* (metastable) form, which is then stabilized in the *trans* form.

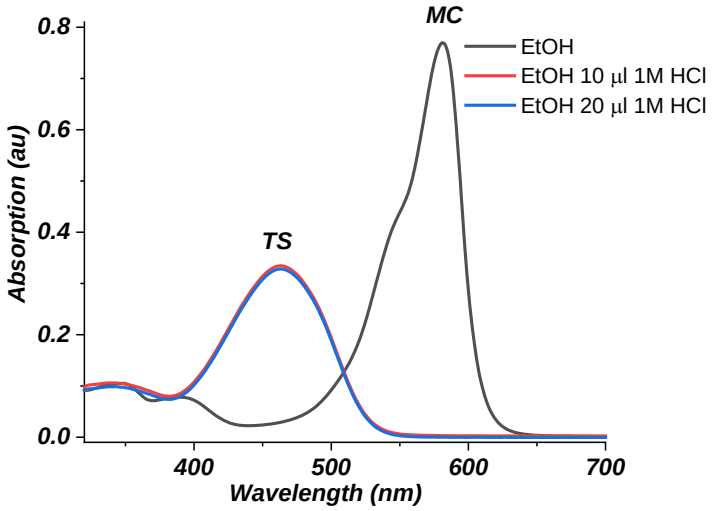

Figure 4. Hydrochloric acid triggered merocyanine to trans-styryl form of dye ***3*** in ethanol.

Irradiation with 450 nm laser light results in a reduction in the *trans* band (463 nm, brown line, Figure 5) and the formation of the *cis* isomer (321 nm, cyan line, Figure 5). In general, the molar absorptivity of the *cis* and *trans* forms does not commensurate. The *cis* form has very low molar absorptivity. After the irradiation, the solution is allowed to relax. The absorbance of the solution was measured every 5 min. As seen from the spectrum in Figure 5, after 24 h, the ***TS*** form is fully restored. The process of transition from merocyanine to the *trans*-styryl form will result in the production of energy when irradiated with light.

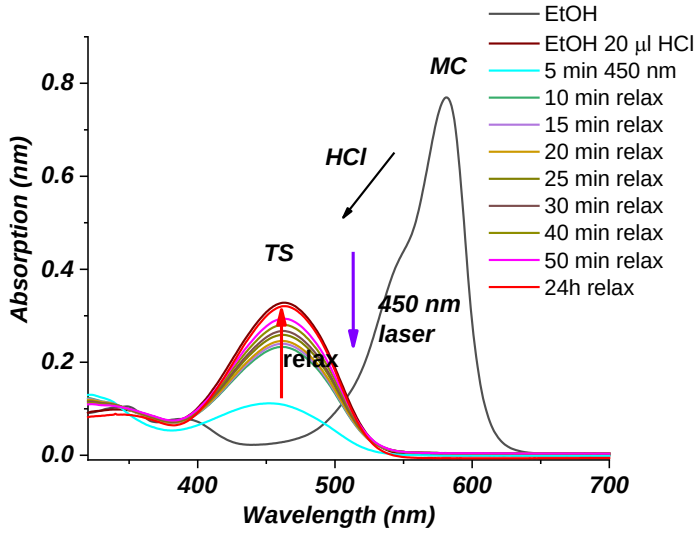

Figure 5. The reversible *cis*-to-*trans* (*Z*-*E*) photoisomerization of photoswitch ***3*** in ethanol–hydrochloric acid system after 5 min 450 nm laser irradiation. Black line: dye ***3*** in ethanol; brown line: dye ***3*** with 20 µL hydrochloric acid added; cyan line: the change after 5 min of irradiation with 450 nm laser light.

The experimental studies were supplemented with PCM [32,33] DFT [34] calculations using B3LYP hybrid functional in conjunction with 6-31G(d,p) [35] basis set, and only the iodine SDD basis set and effective core potential were used [36,37]. The quantum chemical computations were performed with the G16 A.03 software package [38]. The optimized ground state structures and computed relative Gibbs free energies for the dye ***3*** isomers are presented in Figure 6. The optimized structures with iodine counterion are given in Figure S6. The calculated free energies of all the stationary points are reported in kcal/mol relative to the *trans*-styryl form.

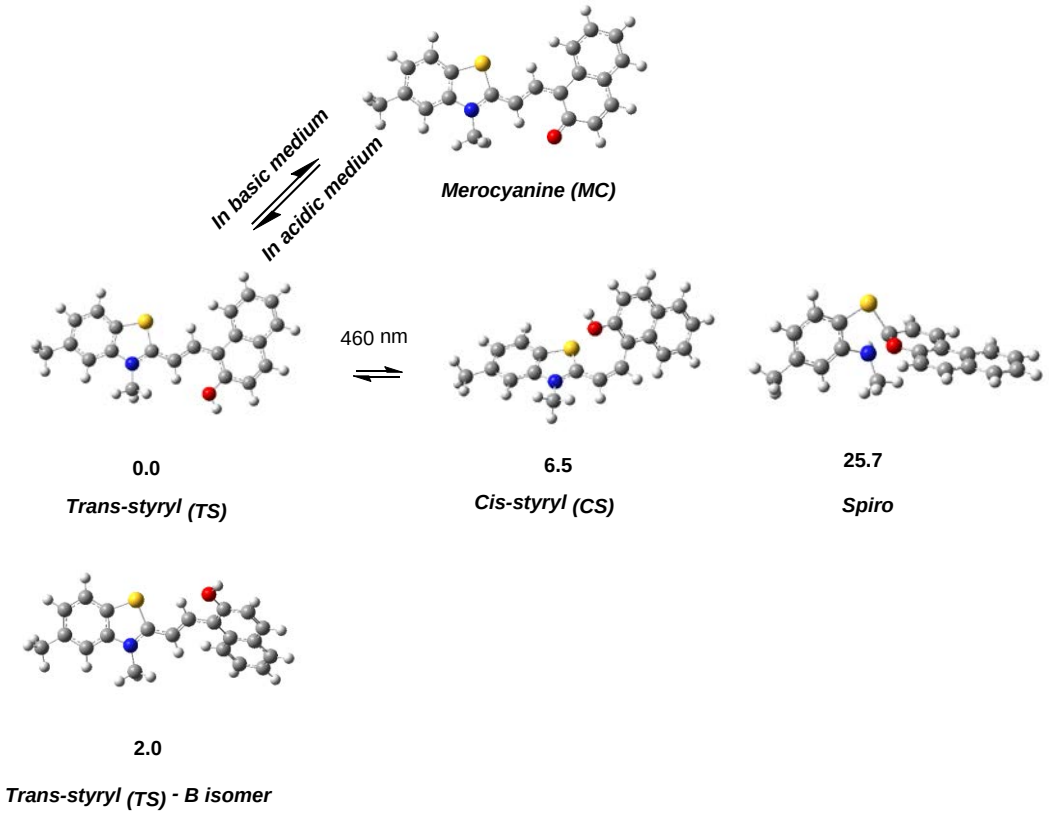

Figure 6. B3LYP/6-31G(d,p) optimized ground state structures (in water medium) and computed relative Gibbs free energies for the dye ***3*** isomers. Color scheme: gray—C, light gray—H, red—O, blue—N, yellow—S.

The Trans-styryl (TS)-B isomer (Figure 6) is more unstable by 2 kcal/mol because the planar structure is disrupted, which lowers the conjugation in the heterocyclic system. The dihedral angle between the benzothiazole and naphthol fragments is 24.15 degrees. Upon irradiation (450 nm), TS converts to the cis isomer (CS). The spiro form is energetically less favorable than the cis form, but its formation cannot be excluded when the system is energized by light irradiation (450 nm). The free energy profile for the transformation between TS, CS, and spiro forms (in water) is presented in Figure 7.

The transition states structures are characterized via the eigenvector of the imaginary frequency and are proven through intrinsic reaction coordinate (IRC) calculations. The spiro form converts to the cis isomer (CS) through an energy barrier of 30.6 kcal/mol. The trans to cis conversion has a free energy barrier of 33.6 kcal/mol (Figure 7). The theoretical results show that the *trans* form is 6.5 kcal/mol more stable than the *cis* form. Therefore, the transition from *cis* to *trans* results in energy gain.

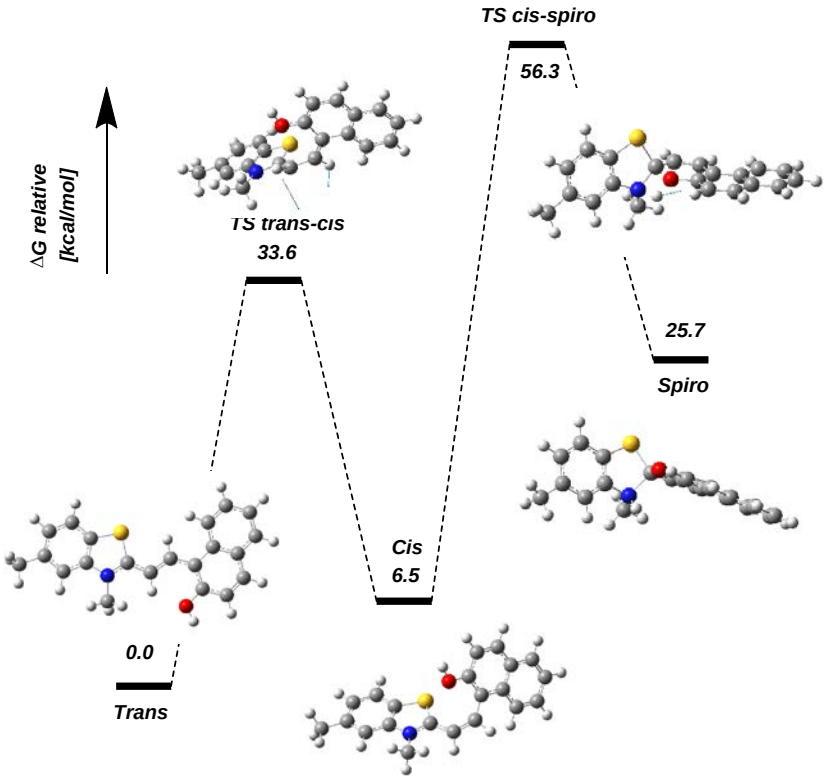

Figure 7. Free energy profile for the transformation between trans (TS), cis (CS), and spiro forms from B3LYP/6-31G(d,p) calculations in water medium. Color scheme: gray—C, light gray—H, red—O, blue—N, yellow—S.

3. Conclusions

The photoswitchable merocyanine dye (*E*)-2-(2-(2-hydroxynaphthalen-1-yl)vinyl)-3,5-dimethylbenzo[*d*]thiazol-3-ium iodide (***3***) was prepared for the first time. The reversible switching between *E* and *Z* isomers and the acidoxchromism of dye ***3*** in DMF and ethanol was studied through the use of UV/Vis spectroscopy and DFT calculations. The *E*-*Z*-isomerization is induced by irradiation with visible light. In an ethanol acidic medium the studied system is suitable for harvesting visible light. The obtained experimental and theoretical results confirm the applicability of the ***TS*** and ***CS*** isomers for proton-triggered light-to-thermal molecular systems. We have a promising candidate, a simple molecule, which is easy to obtain and that can be subsequently modified in order to increase the energy difference between *Z*- and *E*-isomers.

4. Materials and Methods

4.1. General

All of the solvents used in the present work were commercially available (HPLC grade). The synthesis of 2,3,5-trimethylbenzo[*d*]thiazol-3-ium iodide (*1*) was prepared via a previously described procedure [39]. 2-Hydroxy-1-naphthaldehyde (*2*) is commercially available and was used as supplied. The melting points were determined on a Kofler apparatus and were uncorrected. The NMR spectra of the samples in DMSO-d_6 were obtained on a Bruker Avance III 500 DRX 600 MHz spectrometer at the Faculty of Chemistry and Pharmacy, University of Sofia. Mass spectrum acquisitions were conducted at the MPIP, Mainz, Germany on an Advion expression compact mass spectrometer (CMS) with atmospheric pressure chemical ionization (APCI) at high temperature and low fragmentation regime. The MS-spectrum was acquired in the positive ion reflection mode, m/z range from 10 to 1000 m/z, and acquisition speed 10,000 m/z units s^{-1}. The obtained spectrum was analyzed by using Advion CheMS Express software version 5.1.0.2. at the

MPIP, Mainz, Germany. The UV-VIS spectra were measured on a Unicam 530 UV–VIS spectrophotometer in conventional quartz cells of 1 cm path length. The absorption spectra were recorded for solutions with identical total dye concentrations (1×10^{-5} M). A thermal stabilized single-mode diode laser passes through a spatial filter in order to reach nearly TEM_{00} transversal intensity distribution, and the used laser intensity is 1 mW $\times 10^{-2}$ cm, λ = 450 nm, *cw*.

*4.2. Synthesis of (E)-2-(2-(2-Hydroxynaphthalen-1-yl)vinyl)-3,5-dimethylbenzo[d]thiazol-3-ium Iodide (**3**)*

In a 50 mL round bottom flask equipped with an electromagnetic stirrer and reflux condenser, 0.25 g (0.82 mmol) 2,3,5-trimethylbenzo[d]thiazol-3-ium iodide (1) and 0.17 g (0.98 mmol) 2-hydroxy-1-naphthaldehyde (2) were dissolved in 15 mL ethanol and one drop of DIPEA was added. The reaction mixture was vigorously stirred and refluxed under argon for 2 h. After cooling to room temperature, 30 mL of ethyl acetate was added, and the mixture was stored in a refrigerator for 24 h. The formed precipitate was suction filtered, washed with 20 mL cold ethanol and 30 mL ethyl acetate, and air dried. Yield: 0.27 g (71%). M.p. > 250 °C. ^{1}H-NMR (500 MHz, DMSO-d6, δ (ppm)): 2.52 s (3H, CH_3), 4.06 s (3H, CH_3), 7.01 (d, 1H, $^3J_{HH}$ = 9.2 Hz), 7.33 (dd, 1H, $^3J_{HH}$ = 7.3 Hz), 7.46 (d, 1H, CH, $^3J_{HH}$ = 8.4 Hz), 7.55 (dd, 1H, $^3J_{HH}$ = 7.6 Hz), 7.75 (d, 1H, $^3J_{HH}$ = 7.8 Hz), 7.84 (d, 1H, CH, $^3J_{HH}$ = 9.2 Hz), 7.89 (s, 1H, CH), 8.08 (d, 1H, CH, $^3J_{HH}$ = 8.2 Hz), 8.18 (d, 1H, CH, $^3J_{HH}$ = 8.4 Hz), 8.26 (d, 1H, CH, $^3J_{HH}$ = 14.6 Hz), 8.46 (d, 1H, CH, $^3J_{HH}$ = 14.7 Hz). ^{13}C NMR DEPT 125 MHz (DMSO-d_6, δ(ppm)): 21.65 (CH_3), 56.50 (CH_3), 114.01 (CH), 115.77 (CH), 121.91 (CH), 123.56 (CH), 123.87 (CH), 128.55 (CH), 128.69 (CH), 129.55 (CH), 136.33 (CH), 139.59 (CH), 141.49 (CH). Calc. for: $C_{21}H_{18}NOS^+$ m/z = 332.4, found: ESI-MS: m/z = 332.2.

Supplementary Materials: The supporting information can be downloaded at: https://www.mdpi.com/article/10.3390/photochem3020018/s1. Figure S1. 1H-NMR spectrum of dye 3 in DMSO-d6. Figure S2. 1H-NMR spectrum of dye 3 in DMSO-d6—methyl groups region. Figure S3. 1H-NMR spectrum of dye 3 in DMSO-d6—aromatic region. Figure S4. 13C-NMR DEPT spectrum of dye 3 in DMSO-d6. Figure S5. ESI-MS (m/z) spectra of dye 3. Figure S6. B3LYP/6-31G(d,p) optimized ground state structures with iodine counterion (in water medium) and computed relative Gibbs free energies for the dye 3 isomers. Cartesian coordinates of the optimized structures from B3LYP/6-31G** calculations in water medium.

Author Contributions: Conceptualization, S.I., A.A.V., S.B., and D.C.; methodology, S.I. and A.A.V.; validation, S.I., A.A.V., S.B., and D.C.; investigation, A.A.V., S.I., and D.C.; resources, S.I.; data curation, S.I. and D.C.; writing—original draft preparation, S.I. and D.C.; writing—review and editing, A.A.V., S.I., and D.C.; visualization, S.I. and D.C.; supervision, A.A.V. and D.C.; project administration, S.B.; funding acquisition, S.B. All authors have read and agreed to the published version of the manuscript.

Funding: This research was funded by the Bulgarian National Science Fund (BNSF), grant number КП-06-Н37/15-06.12.19 SunUp-project.

Data Availability Statement: The data presented in this study are available either in this article itself and Supplementary Materials.

Conflicts of Interest: The authors declare no conflict of interest.

References

1. Volarić, J.; Szymanski, W.; Simeth, N.A.; Feringa, B.L. Molecular photoswitches in aqueous environments. *Chem. Soc. Rev.* **2021**, *50*, 12377–12449. [CrossRef] [PubMed]
2. Olesińska-Mönch, M.; Deo, C. Small-molecule photoswitches for fluorescence bioimaging: Engineering and applications. *Chem. Commun.* **2023**, *59*, 660–669. [CrossRef] [PubMed]
3. Skov, A.B.; Broman, S.L.; Gertsen, A.S.; Elm, J.; Jevric, M.; Cacciarini, M.; Kadziola, A.; Mikkelsen, K.V.; Nielsen, M.B. Aromaticity-Controlled Energy Storage Capacity of the Dihydroazulene-Vinylheptafulvene Photochromic System. *Chem. Eur. J.* **2016**, *22*, 14567. [CrossRef] [PubMed]

4. Mogensen, J.; Christensen, O.; Kilde, M.D.; Abildgaard, M.; Metz, L.; Kadziola, A.; Jevric, M.; Mikkelsen, K.V.; Nielsen, M.B. Molecular Solar Thermal Energy Storage Systems with Long Discharge Times Based on the Dihydroazulene/Vinylheptafulvene Couple. *Eur. J. Org. Chem.* **2019**, *2019*, 1986–1993. [CrossRef]
5. Moth-Poulsen, K.; Ćoso, D.; Börjesson, K.; Vinokurov, N.; Meier, S.K.; Majumdar, A.; Vollhardt, K.P.C.; Segalman, R.A. Molecular solar thermal (MOST) energy storage and release system. *Energy Environ. Sci.* **2012**, *5*, 8534–8537. [CrossRef]
6. Bren', V.A.; Dubonosov, A.D.; Minkin, V.I.; Chernoivanov, V.A. Norbornadiene–quadricyclane—An effective molecular system for the storage of solar energy. *Russ. Chem. Rev.* **1991**, *60*, 451–469. [CrossRef]
7. Bandara, H.M.D.; Burdette, S.C. Photoisomerization in different classes of azobenzene. *Chem. Soc. Rev.* **2012**, *41*, 1809–1825. [CrossRef]
8. Velema, W.A.; Szymanski, W.; Feringa, B.L. Photopharmacology: Beyond Proof of Principle. *J. Am. Chem. Soc.* **2014**, *136*, 2178–2191. [CrossRef]
9. Dong, L.; Feng, Y.; Wang, L.; Feng, W. Azobenzene-based solar thermal fuels: Design, properties, and applications. *Chem. Soc. Rev.* **2018**, *47*, 7339–7368. [CrossRef]
10. Shi, Y.; Gerkman, M.A.; Qiu, Q.; Zhang, S.; Han, G.G.D. Sunlight-activated phase change materials for controlled heat storage and triggered release. *J. Mater. Chem. A* **2021**, *9*, 9798–9808. [CrossRef]
11. Qiu, Q.; Shi, Y.; Han, G.G.D. Solar energy conversion and storage by photoswitchable organic materials in solution, liquid, solid, and changing phases. *J. Mater. Chem. C* **2021**, *9*, 11444–11463. [CrossRef]
12. Volarić, J.; Thallmair, S.; Feringa, B.L.; Szymanski, W. Photoswitchable, Water-Soluble Bisazobenzene Cross-Linkers with Enhanced Properties for Biological Applications. *ChemPhotoChem* **2022**, *6*, e202200170. [CrossRef]
13. Matsuda, K.; Irie, M. Diarylethene as a photoswitching unit. *J. Photochem. Photobiol. C* **2004**, *5*, 169–182. [CrossRef]
14. Kudernac, T.; van der Molen, S.J.; van Wees, B.J.; Feringa, B.L. Uni- and bi-directional light-induced switching of diarylethenes on gold nanoparticles. *Chem. Commun.* **2006**, *34*, 3597–3599. [CrossRef]
15. Broichhagen, J.; Frank, J.A.; Trauner, D. A Roadmap to Success in Photopharmacology. *Acc. Chem. Res.* **2015**, *48*, 1947–1960. [CrossRef]
16. Lerch, M.M.; Hansen, M.J.; van Dam, G.M.; Szymanski, W.; Feringa, B.L. Emerging Targets in Photopharmacology. *Angew. Chem. Int. Ed.* **2016**, *55*, 10978–10999. [CrossRef]
17. Fischer, E.; Hirshberg, Y. Formation of Coloured Forms of Spirans by Low-Temperature Irradiation. *J. Chem. Soc.* **1952**, 4522–4524. [CrossRef]
18. Klajn, R. Spiropyran-based dynamic materials. *Chem. Soc. Rev.* **2014**, *43*, 148–184. [CrossRef]
19. Hu, D.H.; Tian, Z.Y.; Wu, W.W.; Wan, W.; Li, A.D.Q. Single-Molecule Photoswitching Enables High-Resolution Optical Imaging. *Microsc. Microanal.* **2009**, *15*, 840–841. [CrossRef]
20. Tian, Z.Y.; Li, A.D.Q.; Hu, D.H. Super-resolution fluorescence nanoscopy applied to imaging core–shell photoswitching nanoparticles and their self-assemblies. *Chem. Commun.* **2011**, *47*, 1258–1260. [CrossRef]
21. Montagnoli, G.; Pieroni, O.; Suzuki, S. Control of peptide chain conformation by photoisomerising chromophores: Enzymes and model compounds. *Polym. Photochem.* **1983**, *3*, 279–294. [CrossRef]
22. Ciardelli, F.; Fabbri, D.; Pieroni, O.; Fissi, A. Photomodulation of polypeptide conformation by sunlight in spiropyran-containing poly(L-glutamic acid). *J. Am. Chem. Soc.* **1989**, *111*, 3470–3472. [CrossRef]
23. Sakata, T.; Yan, Y.L.; Marriott, G. Optical switching of dipolar interactions on proteins. *Proc. Natl. Acad. Sci. USA* **2005**, *102*, 4759–4764. [CrossRef] [PubMed]
24. Fissi, A.; Pieroni, O.; Angelini, N.; Lenci, F. Photoresponsive Polypeptides. Photochromic and Conformational Behavior of Spiropyran-Containing Poly-l-Glutamate)s under Acid Conditions. *Macromolecules* **1999**, *32*, 7116–7121. [CrossRef]
25. Wojtyk, J.T.C.; Wasey, A.; Xiao, N.N.; Kazmaier, P.M.; Hoz, S.; Yu, C.; Lemieux, R.P.; Buncel, E. Elucidating the Mechanisms of Acidochromic Spiropyran-Merocyanine Interconversion. *J. Phys. Chem. A* **2007**, *111*, 2511–2516. [CrossRef]
26. Remon, P.; Li, S.M.; Grotli, M.; Pischel, U.; Andreasson, J. An Acido- and Photochromic Molecular Device That Mimics Triode Action. *Chem. Commun.* **2016**, *52*, 4659–4662. [CrossRef]
27. Schmidt, S.B.; Kempe, F.; Brügner, O.; Walter, M.; Sommer, M. Alkyl-Substituted Spiropyrans: Electronic Effects, Model Compounds and Synthesis of Aliphatic Main-Chain Copolymers. *Polym. Chem.* **2017**, *8*, 5407–5414. [CrossRef]
28. Roxburgh, C.J.; Sammes, P.G. On the Acid Catalysed Isomerisation of Some Substituted Spirobenzopyrans. *Dyes Pigments* **1995**, *27*, 63–69. [CrossRef]
29. Shiozaki, H. Molecular Orbital Calculations for Acid Induced Ring Opening Reaction of Spiropyran. *Dyes Pigments* **1997**, *33*, 229–237. [CrossRef]
30. Kortekaas, L.; Chen, J.; Jacquemin, D.; Browne, W.R. Proton-Stabilized Photochemically Reversible *E*/*Z* Isomerization of Spiropyrans. *J. Phys. Chem. B* **2018**, *122*, 6423–6430. [CrossRef]
31. Vasilev, A.; Dimitrova, R.; Kandinska, M.; Landfester, K. Baluschev. S. Accumulation of the photonic energy of the deep-red part of the terrestrial sun irradiation by rare-earth metal-free E–Z photoisomerization. *J. Mater. Chem. C* **2021**, *9*, 7119–7126. [CrossRef]
32. Cossi, M.; Barone, V.; Cammi, R.; Tomasi, J. Ab initio study of solvated molecules: A new implementation of the polarizable continuum model. *Chem. Phys. Lett.* **1996**, *255*, 327–335. [CrossRef]
33. Tomasi, J.; Mennucci, B.; Cammi, R. Quantum Mechanical Continuum Solvation Models. *Chem. Rev.* **2005**, *105*, 2999–3094. [CrossRef]

34. Labanowski, J.K.; Andzelm, J.W. (Eds.) *Density Functional Methods in Chemistry*; Springer: New York, NY, USA, 1991.
35. Petersson, G.A.; Bennett, A.; Tensfeldt, T.G.; Al-Laham, M.A.; Shirley, W.A.; Mantzaris, J. A complete basis set model chemistry. I. The total energies of closed-shell atoms and hydrides of the first-row elements. *J. Chem. Phys.* **1988**, *89*, 2193–2218. [CrossRef]
36. Leininger, T.; Nicklass, A.; Stoll, H.; Dolg, M.; Schwerdtfeger, P. The accuracy of the pseudopotential approximation. II. A comparison of various core sizes for indium pseudopotentials in calculations for spectroscopic constants of InH, InF, and InCl. *J. Chem. Phys.* **1996**, *105*, 1052–1059. [CrossRef]
37. Haas, J.; Bissmire, S.; Wirth, T. Iodine Monochloride–Amine Complexes: An Experimental and Computational Approach to New Chiral Electrophiles. *Chem. Eur. J.* **2005**, *11*, 5777–5785. [CrossRef]
38. Frisch, M.J.; Trucks, G.W.; Schlegel, H.B.; Scuseria, G.E.; Robb, M.A.; Cheeseman, J.R.; Scalmani, G.; Barone, V.; Petersson, G.A.; Nakatsuji, H.; et al. *Gaussian 16 Revision 16.A.03*; Gaussian, Inc.: Wallingford, CT, USA, 2016.
39. Zonjić, I.; Radić Stojković, M.; Crnolatac, I.; Tomašić Paić, A.; Pšeničnik, S.; Vasilev, A.; Kandinska, M.; Mondeshki, M.; Baluschev, S.; Landfester, K.; et al. Styryl dyes with N-Methylpiperazine and N-Phenylpiperazine Functionality: AT-DNA and G-quadruplex binding ligands and theranostic agents. *Bioorg. Chem.* **2022**, *127*, 105999. [CrossRef]